
Benchmarking procedures for high-throughput context specific reconstruction algorithms

Maria Pires Pacheco¹, Thomas Pfau^{1,2} and Thomas Sauter^{1*},

¹*Life Sciences Research Unit, University of Luxembourg, L-1511 Luxembourg, Luxembourg*

²*Institute of Complex Systems and Mathematical Biology, University of Aberdeen, AB24 3UE Aberdeen, United Kingdom*

Correspondence*:

Thomas Sauter

Life Sciences Research Unit, University of Luxembourg, L-1511 Luxembourg, Luxembourg, thomas.sauter@uni.lu

2 ABSTRACT

3 Recent progress in high-throughput data acquisition has shifted the focus from data generation
4 to processing and understanding of how to integrate collected information. Context specific
5 reconstruction based on generic genome scale models like ReconX or HMR has the potential
6 to become a diagnostic and treatment tool tailored to the analysis of specific individuals. The
7 respective computational algorithms require a high level of predictive power, robustness and
8 sensitivity. Although multiple context specific reconstruction algorithms were published in the last
9 ten years, only a fraction of them is suitable for model building based on human high-throughput
10 data. Beside other reasons, this might be due to problems arising from the limitation to only one
11 metabolic target function or arbitrary thresholding.

12 This review describes and analyses common validation methods used for testing model building
13 algorithms. Two major methods can be distinguished: consistency testing and comparison
14 based testing. The first is concerned with robustness against noise, e.g. missing data due to
15 the impossibility to distinguish between the signal and the background of non-specific binding
16 of probes in a microarray experiment, and whether distinct sets of input expressed genes
17 corresponding to i.e. different tissues yield distinct models. The latter covers methods comparing
18 sets of functionalities, comparison with existing networks or additional databases. We test those
19 methods on several available algorithms and deduce properties of these algorithms that can
20 be compared with future developments. The set of tests performed, can therefore serve as a
21 benchmarking procedure for future algorithms.

22 **Keywords:** Metabolic Networks and Pathways; Metabolic Reconstruction; Constraint-based modelling; Tissue Specific Networks;
23 **Benchmarking; Validation**

1 INTRODUCTION

24 Metabolic network reconstructions become ever more complicated and complete with reconstructions
25 like Recon2 (Thiele et al., 2013) or HMR (Mardinoglu et al., 2014) containing more than 7000 reactions.
26 While these reconstructions are a great tool for the analysis of the potential capabilities of an organism, one
27 challenge faced by many researchers is that different cell types in multicellular organisms exhibit diverse
28 functionality and the global generic network is too flexible. This issue has been addressed in two ways, by
29 manually generating tissue specific models (Gille et al., 2010; Quek et al., 2014) or by creating algorithms
30 for automatic reconstructions (Becker and Palsson, 2008; Zur et al., 2010; Jerby et al., 2010; Agren et al.,
31 2012; Wang et al., 2012; Vlassis et al., 2014; Yizhak et al., 2014; Robaina Estévez and Nikoloski, 2015).
32 Ryu et al. (2015) and Robaina Estévez and Nikoloski (2014) recently reviewed this field and give a good
33 overview of the available reconstructions and point to many algorithms used in this context. While Ryu et al.
34 (2015) are more concerned with the the state of the reconstructions, Robaina Estévez and Nikoloski (2014)
35 focused on the applicability and properties of the available algorithms. With that many methods available,
36 the method selection is difficult, and it is an enormous effort to try and distinguish which network, of a set
37 of generated networks is best. Quality assessment is therefore essential but the methods used to evaluate the
38 currently available algorithms are very diverse and it is difficult to compare them with each other. There are
39 several approaches for validation which can essentially be split into two different categories: Consistency
40 testing and Comparison based testing. The first is concerned with robustness against noise, e.g. missing
41 data, and whether distinct sets of input data yield distinct models. The second commonly aims at validating
42 the resulting model against other models or against additional data. Comparison tends to be the more
43 common approach so far, while consistency is often ignored. This leads to the problem that algorithms are
44 often prone to be over-specific to the comparison dataset (e.g. parameters like expression thresholds or
45 weights working well for only one specific tissue). While comparison methods validate the reconstructed
46 model, they are however not validating the consistency. Thus, it is possible that small differences in the
47 input dataset can lead to vastly different networks, or even very diverse datasets yield the same models.
48 The latter is particularly true if e.g. a biomass function is set as objective function, since it will lead to the
49 inclusion of a multitude of reactions, which might not be necessary if a specific tissue is supplied with
50 some metabolites by other tissues. To investigate the quality of automatically reconstructed networks it is
51 therefore necessary to rigorously test them. In the following paragraphs, we describe multiple methods that
52 were used in the past. Table 1 also gives an overview of these approaches, and details which concept was
53 used for validation of which algorithm.

54 1.1 Methods for testing algorithmic consistency

55 The idea of consistency testing covers two major aspects: Robustness of the method and its capacity to
56 distinguish slightly different contexts.

57 If feasible, random cross validation of the resulting models for a given set of input data can help to
58 determine the robustness of the method with respect to noisy data (Vlassis et al., 2014). Left-out cross-
59 validation allows identifying the reactions that if left-out from the input set would nevertheless be included
60 (or excluded for inactive reactions) in the output model as their inclusion is supported by other reactions of
61 the input set (Pacheco et al., 2015). The robustness of algorithms against noise can also be assessed by
62 adding noise to the expression data i.e. by using a weighted combination of real and random data (Machado
63 and Herrgård, 2014). The main issue using random and left-out cross validation with most of the current
64 algorithms is that running times of several hours makes decent cross-validation with hundreds of test and
65 validation sets infeasible. While small cross validation runs (e.g. when multiple sources of input data are

66 available and only some sets are considered (Jerby et al., 2010)) can give an indication of robustness, they
67 cannot replace random sampling runs, which reflect noisy data much better.

68 To test the diversity of generated networks, many algorithms are employed to generate multiple networks
69 and those networks are then investigated for dissimilarity (Becker and Palsson, 2008; Wang et al., 2012;
70 Uhlén et al., 2015; Agren et al., 2014; Pacheco et al., 2015). If networks of similar cell types group together
71 in a clustering and networks of divergent cell types are further apart, this indicates that the method does
72 indeed generate specific networks. While it is desirable to obtain distinct networks for distinct tissues, the
73 optimal method should not be too sensitive to small changes in the input data. Otherwise the resulting
74 networks are prone to overfitting to the provided input data.

75 1.2 Methods for comparison based testing

76 Comparison based testing is commonly employed to show the advantages of the presented algorithm
77 compared over previous algorithms or to show the quality of the reconstructed network based on additional,
78 formerly unknown, data. While the former has been employed for the validation of some algorithms (Wang
79 et al., 2012; Vlassis et al., 2014; Robaina Estévez and Nikoloski, 2015), and becomes more important with
80 an increasing number of available methods, it has also recently been used to compare multiple methods
81 systematically (Machado and Herrgård, 2014; Robaina Estévez and Nikoloski, 2014). In the review by
82 Machado and Herrgård (2014) 8 different methodologies (including GIMME (Becker and Palsson, 2008),
83 iMAT (Zur et al., 2010) and a Method by Lee et al. (2012)) were tested on an independent dataset.
84 However, their focus was on comparing the quality of flux value predictions, i.e. flux bounds specific to
85 a condition in *Escherichia coli* and yeast, and not the reconstruction of tissue specific networks, i.e. the
86 extraction of an active sub-network.

87 1.2.1 Comparison against manually curated networks

88 Comparison to a manually curated tissue was employed by Agren et al. (2012) for the INIT algorithm,
89 when they compared their automatically generated liver reconstruction to HepatoNet. However, they
90 were restricted to a comparison on the gene level, since the source network used by INIT was the
91 HMR database (Mardinoglu et al., 2013), while HepatoNet used its own identifiers. As they mention the
92 difference between the reconstructed and manually curated models was partially due to absence of genes
93 from HMR that were present in HepatoNet. Simultaneously, it is likely that the curators of HepatoNet
94 lacked information on some of the genes present in HMR. Thus to validate a methodology it is necessary
95 for both the “reference” network and the source network to be compatible.

96 1.2.2 Comparison against additional datasets and databases

97 Similarly, many methods compare the resulting reconstructions to additional databases that contain tissue
98 localisation data (like BRENDA (Schomburg et al., 2013), HPA (Uhlén et al., 2015) or the Gene Expression
99 Omnibus (Barrett et al., 2013)), which was performed for multiple reconstruction methods (Shlomi et al.,
100 2008; Wang et al., 2012; Robaina Estévez and Nikoloski, 2015). The common approach is to check for
101 matches of either genes or proteins that the algorithm assigned to the tissue. This validation (and the
102 results) are however highly dependent on whether the reconstruction method aims at creating a consistent
103 network, or whether it allows inconsistent reactions to be part of the reconstruction. The latter will very
104 likely increase the amount of correctly assigned genes, as enzymatic activities that cannot carry flux in
105 the source reconstruction, would otherwise be excluded. In addition, when extracting reactions from a
106 source network, the associated gene-protein reaction relations are commonly not altered. Thus genes,
107 which are inactive in a specific tissue show up as assigned to the tissue. Removing them however, could

108 potentially be problematic if the tissue does express the removed gene under a specific condition. In this
109 instance the tissue reconstruction would no longer contain information about this fact, and would indicate
110 wrong potentials of the tissue. Another method that could be used as an assessment for predictive quality
111 of an algorithm was performed by Folger et al. (2011) and subsequently by Pacheco et al. (2015). They
112 used gene silencing data from an shRNA screen and compared it with gene essentiality predictions from
113 a flux balance analysis (FBA) analysis screen. The cancer network generated in this work showed an
114 enrichment of essential genes in the genes indicated in the shRNA screen. In Pacheco et al. (2015), the
115 list of essential genes predicted by FASTCORMICS was further compared to essential genes predicted
116 by PRIME, MBA, mCADRE and GIMME. Likewise bibliographic approaches have been employed to
117 determine the agreement of reactions belonging to a certain subsystem in the reconstructed network and
118 those subsystems being mentioned in connection with the reconstructed tissue in the literature (Shlomi
119 et al., 2008).

120 To assess the predictive capability of the Model Building Algorithm (MBA) Jerby et al. (2010) used
121 flux data from a study performed in primary rat hepatocytes and compared the ability of the source
122 reconstruction and the generated reconstruction to predict internal fluxes given the exchange fluxes (and
123 vice versa). This allowed them to assess whether the tissue specific network was indeed performing better
124 in estimating the internal fluxes than the generic reconstruction (in this instance Recon1). They could
125 show that indeed the tissue specific network had a better capability to capture the actual fluxes than the
126 generic reconstruction. This concept was also used by Machado and Herrgård (2014) in their assessment
127 of multiple methods for network contextualisation. However, while contextualisation commonly aims at
128 altering flux bounds, which leads to a good comparability of flux measurements with predictions, tissue
129 specific reconstruction is aiming at determining the network available in a given tissue. This means that
130 bounds from the underlying source reconstruction are used and these are often unsuitable for the tissue
131 of interest. But as shown by Jerby et al. (2010), even the pure network structure alteration can already
132 improve the agreement between network fluxes and measured data, at least on a qualitative level.

133 A method developed by Shlomi et al. (2009) to compare the resulting network for the effects of inborn
134 errors of metabolism (IEM) is also often used in model quality assessment. The concept is, briefly, to
135 analyse flux ranges of the exchange reactions of the created network and compare them with clinical
136 indications of increased or decreased metabolite levels. This concept has also been used for assessment of
137 Recon2 (Thiele et al., 2013) who investigated a diverse set of IEMs and could show their effect even on the
138 level of a generic reconstruction. Similarly, the authors of PRIME (Yizhak et al., 2014) used experimentally
139 measured uptake and excretion rates and compared them to the secretion rates determined by the models
140 their algorithm generated. While the former approach is commonly used to provide a qualitative assessment
141 of increase or decrease in production potential, the latter results in a quantitative comparison. However, it
142 requires the availability of uptake and secretion rates, which are commonly only available for cell lines and
143 could be largely different in real tissues.

144 Another common approach to investigate the quality of reconstructions is the comparison with lists of
145 metabolic functions. This approach is both used to validate automated reconstructions (Jerby et al., 2010;
146 Wang et al., 2012) as well as manual reconstructions (Gille et al., 2010). The aim is to establish whether the
147 reconstruction supports the current knowledge of the target tissue (e.g. a liver reconstruction should support
148 the conversion of ammonia to urea), and to show that there are no structural issues in the reconstructed
149 network (e.g. free regeneration of ATP or reductants).

150 1.3 A benchmark for testing tissue specific reconstruction algorithms

151 In this paper we present a potential benchmark that is using several of the mentioned methodologies to
152 assess the consistency and quality of reconstructed networks and tested it with several of the available
153 algorithms.

154 There are however multiple obstacles, when defining a benchmark for contextualisation algorithms. There
155 is no such thing as a “perfect” measurement, which will always leave us with noisy data to incorporate.
156 Furthermore, we do not yet have a contextualised model that perfectly reflects a given context which could
157 be used as a target model. In addition, the global reconstructions are not yet complete, and will likely never
158 be and finally, there is a wide variety of data that can be used to contextualise models. Thus, to define a
159 benchmark we will address these questions by generating networks which we define as reference networks
160 for out testing.

161 The actual benchmark is preceded by a characterization of the algorithms, in which the similarity level of
162 the context-specific reconstructions obtained with real and artificial input data is assessed. In the latter test,
163 artificial models of different sizes were built and 50%, 60%, 70%, 80% and 90% of the reactions of these
164 networks were used as input for the tested algorithms. The capacity of the algorithm to distinguish between
165 different models was compared for the different percentages of input data.

166 In the actual benchmark, the confidence level of the reactions included in the context-specific
167 reconstructions using real data was assessed by matching z-scores obtained by the Barcode (McCall
168 et al., 2011) method that basically indicate the difference in intensity between the measured intensity and
169 the intensity distribution observed in an unexpressed state and through a comparison against the confidence
170 score at the proteomic level of the Human Protein Atlas (Uhlén et al., 2015). In a second comparison,
171 artificial models were built and 50%, 60%, 70%, 80% and 90% of the reactions of these networks were
172 used as input for the tested algorithms and the output models were then compared to the complete input
173 model. The context-specific networks obtained with the real data were also tested for the functionalities
174 established by (Gille et al., 2010).

2 MATERIAL & METHODS

175 2.1 Models used for Benchmarking

176 There are currently two competing global reconstructions for humans available: Recon2 (Thiele et al.,
177 2013) and HMR2 (Mardinoglu et al., 2013). To be able to test multiple validation techniques, we needed
178 to select one of those reconstructions as the source network used by the tested algorithms. We decided
179 to employ Recon2, as we used functionalities originating from HepatoNet (Gille et al., 2010), a model
180 based on Recon1 (Duarte et al., 2007) and largely incorporated into Recon2. However we still had to
181 modify Recon2 to allow the algorithms to fully reconstruct HepatoNet (the procedure can be found in
182 Supplementary File 1). HepatoNet was also adapted to match reactions and metabolites with Recon2. This
183 modified Recon2 was used as source model for all runs.

184 In addition to HepatoNet as a comparison model for real data, we constructed ten artificial sub-networks
185 from Recon2. Those networks were generated to be approximately equally spaced in a range between 1000
186 and 3500 reactions. They were generated by randomly removing up to 4500 reactions from our Recon2
187 version and determining the consistent part of the remaining model. The first model within ± 50 reactions
188 of equally spaced points in the interval [1000..3500] was selected as representative for this point. The
189 models and model sizes can be found Supplementary File 5.

190 2.2 Characterization of the algorithms

191 There are many algorithms available for tissue-specific metabolic network reconstructions (see Table 2).
192 In this section we will detail the algorithms used in our study and give reasons, why others were excluded.

193 In order to test the algorithms with real data, liver models were built by the tested algorithms using as
194 input 22 arrays from different datasets downloaded from the Gene Expression Omnibus (GEO) (Edgar
195 et al., 2002) database (Supplementary File 2). The same data was also used for the cross-validation assays.

196 2.2.1 GIMME (Becker and Palsson, 2008) and iMAT (Zur et al., 2010)

197 For the benchmarking of the GIMME (Becker and Palsson, 2008) and the iMAT (Zur et al., 2010)
198 algorithms, the implementation provided by the COBRA toolbox (Schellenberger et al., 2011) was used
199 with an expression threshold corresponding to the 75th percentile. The proceedExp option was set to 1 as
200 the data was preprocessed. For GIMME, the biomass objective coefficient was set to 10^{-4} .

201 2.2.2 INIT (Agren et al., 2012)

202 In the original paper, INIT (Agren et al., 2012) assigns weights to the genes associated to the input model
203 that were computed by dividing the gene expression in the tissue of interest by the average expression
204 across all tissues. As for the first experiment, only liver arrays were available, z-scores obtained by the
205 Barcode (Zilliox and Irizarry, 2007; McCall et al., 2011) discretization method, were used as weights (see
206 below).

207 2.2.3 RegrEx (Robaina Estévez and Nikoloski, 2015)

208 The RegrEx implementation in the supplementary files of (Robaina Estévez and Nikoloski, 2015) was
209 used. This algorithm has previously only been used with RNA-seq data and therefore no established
210 discretization method exist for microarray data. In order to allow a comparison with the others methods, the
211 intensity values after frma normalization and the standard variation were directly mapped to the reactions
212 of the model using the Gene-Protein-Reaction rules (GPR). For reactions that are not associated to any
213 gene, the expression and the standard deviation were set to 0 and 1000 respectively.

214 2.2.4 Akesson (Åkesson et al., 2004)

215 For this algorithm, the data was normalized with the frma normalization method and then discretized
216 with Barcode. Genes with z-scores below 0 in 90% of the arrays, were considered inactive and the bounds
217 of the associated reactions, taking into account the Gene-Protein-Reaction rules (GPR), were set to 0.
218 FASTCC (Vlassis et al., 2014) was then run to remove reactions that are unable to carry a flux.

219 2.2.5 FASTCORE z-score

220 For FASTCORE z-score, the expression data was normalized with frma method and discretized using
221 Barcode. Barcode uses previous knowledge on the intensity distribution across thousands of arrays to
222 calculate for each probe set of the analysed array the number of standard deviations to the median of the
223 intensity distribution for the same probe set in an unexpressed state. Genes with a z-score above 5 in 90%
224 of arrays are considered as expressed and mapped to the reactions according to the Gene-Protein-Reaction
225 rules (GPR) to obtain a core set that is fed into FASTCORE (Vlassis et al., 2014).

226 2.2.6 FASTCORMICS (Pacheco et al., 2015)

227 The expression values were first normalized with frma, converted into z-scores using Barcode (McCall
228 et al., 2011) and further discretized using an expression threshold of 5 z-scores and an unexpression

229 threshold of 0 z-score. Genes with 90% of the arrays above the expression threshold are assigned a score of
230 1 while those below the unexpression threshold are assigned a score of -1. All other genes are associated
231 with a discretization score of 0. These scores are then mapped onto the model using the Gene-Protein-
232 Reactions rules to obtain lists of core and unexpressed reactions. Unexpressed reactions are excluded from
233 the model.

234 The FASTCORMICS workflow allows the inclusion of a medium composition, which was not used in the
235 tests, as the aim was to provide the same information to all algorithms. A modified version of FASTCORE
236 is then run that maximizes the inclusion of core reactions while penalizing the entry of non core reactions.
237 Note that transporter reactions are excluded from the core set but are not penalized.

238 2.2.7 Context-specific reconstruction algorithm that were not tested

239 PRIME and tINIT were not included in the tests as they require, in addition to expression data, growth
240 rates for PRIME and information on tissue functionalities for tINIT. Determination of growth rates in
241 multicellular organisms is restricted to cell lines or cancerous cells, as most other cell types are finally
242 differentiated and therefore no longer divide. Since growth rates are an essential part of PRIME it was
243 excluded from the tests. While functionalities are available for some metabolically very active tissues (like
244 kidney and liver), they are often not available for others. Since we wanted to test a wide range of potential
245 tissues, we decided not to employ functionalities in our input set. Therefore tINIT would be reduced to
246 INIT as the remaining functionality is the same. Since we wanted to focus on gene expression data, which
247 is currently the most readily available type of data, we did not add metabolomic information into our
248 screens. GIM³E would need this type of information and was therefore not tested. Finally, MBA, Lee
249 and mCADRE took more than 5 days for a single run on 2 cores of our cluster and where therefore not
250 included.

251 2.2.8 Similarity of the context-specific models and algorithm-related bias

252 The similarity level between the context-specific models built by the tested algorithms was assessed by
253 computing the Jaccard index between each pair of models. The matrix containing the Jaccard indices was
254 then clustered using Euclidian distance. Further, for each context-specific model, the number of reactions
255 found by only 1, 2 up to all of the methods was computed and represented as a stacked boxplot. The
256 coloured areas represent the different models built by the tested algorithms and for each bin the coloured
257 area is proportional to the number of shared reactions.

258 2.2.9 Sensitivity and Robustness testing using artificial data

259 While there are methods that take continuous expression measurements into account (Colijn et al., 2009;
260 Lee et al., 2012) (and reviewed in (Machado and Herrgård, 2014)), other methods require the user to define
261 sets of reactions that are present (FASTCORE, MBA) or perform some form of discretization to determine
262 the presence or absence of a gene or a reaction (Akesson, GIMME, iMAT, FASTCORMICS). The latter
263 types of methods, using some form of presence/absence calls can be more rigorously tested for robustness,
264 as a target model can be used to provide the present and absent genes/reactions.

265 We also tested these algorithms using the artificially created networks. The test was performed as follows:
266 The potential available information was defined as the sets of reactions present in each submodel and absent
267 from each submodel. Based on this data different percentages of input information (50%, 60%, 70%, 80%,
268 90%) were provided to the algorithms. The same random samples were provided to the tested algorithms to
269 allow a further comparison between the algorithms (generating a total of 5000 models for each algorithm).
270 To be able to use reaction data, we modified the implementation of the GIMME algorithm to allow the

271 direct provision of the *ExpressedRxns* and *UnExpressedRxns* fields. The model similarities were assessed
272 by calculating the Jaccard index between each pair of models generated for input sets from different target
273 models. In addition, the internal distances of all models generated for one target model were calculated (a
274 total of 50000 comparisons per algorithm). Furthermore, the corresponding models for each algorithm and
275 each tested input percentage were compared, to obtain the inter-algorithm distance.

276 2.2.10 Robustness testing using real data

277 For the cross-validation, 20% of the reactions were removed from the core set and transferred to the
278 validation set. The number of these reactions that were included in the output model was determined and
279 a hypergeometric test was computed. The process was repeated 100 times randomizing at each iteration
280 the core set to form different validation sets. For algorithms that take continuous data as input, the cross-
281 validation assay was adapted as follows: 20% of the gene-associated reactions were removed from the input
282 set by setting the expression to 0 and the standard deviation to 1000 for RegrEX and the rxnsScores to 0
283 for INIT. But only reactions considered to be expressed with a high confidence level formed the validation
284 set i.e. for INIT only reaction with z-scores above 5 and with expression value above 10 for RegrEX. For
285 Akesson the validation set was composed of inactive reactions. The results for Akesson have to be taken
286 with care as the validation set is only composed of 4 reactions. This is due to Barcode only indicating very
287 few genes as absent, which led to only about 40 reactions being removed from Recon2.

288 2.3 Benchmarking with real data

289 2.3.1 Confidence level of the reactions

290 The z-scores computed by Barcode translate the number of standard deviations to the intensity distribution
291 of the same genes in an unexpressed state. The z-scores of the genes were mapped to the reactions of
292 Recon2 (Thiele et al., 2013), HepatoNet (Gille et al., 2010) and to the context-specific models built by the
293 different workflows using the Gene Protein Rules (GPR). In the same way, the confidence levels assigned
294 by the Human Protein Atlas (HPA) to the proteins of the database were mapped to the reactions of the
295 different context-specific models.

296 2.3.2 Comparison between different tissue models

297 The aptitude of the algorithm to capture metabolic variations among tissues was tested using the GSE2361
298 dataset (Ge et al., 2005) downloaded from Gene Expression Omnibus (GEO) that contains 36 types of
299 normal human tissues. 21 of the 36 tissues matched tissues in the Human Protein Atlas. The confidence
300 levels of the proteins in the different tissues were first matched to the modified version of Recon2 to
301 determine if proteins with high and medium confidence level are ubiquitously expressed or expressed in a
302 more tissue specific manner. Then the confidence levels were matched to the corresponding context-specific
303 models to verify if the variation observed among the tissue context-specific models matched the one
304 observed in the Human Protein Database.

305 To further assess the quality of the reconstructed models, the fraction of reactions of the Recon2 pathways
306 that are active in the output models were computed. The obtained matrix was then clustered in function of
307 the Euclidean distance (see Supplementary Figure 6.)

308 2.4 Benchmarking with artificial data

309 The runs using artificial data, performed for sensitivity and robustness analysis, were also used to provide
310 an additional benchmarking measurement for the algorithms. Sensitivity and specificity and false discovery

311 rate were calculated by comparison of the reconstructed networks with the respective target network. The
 312 artificial nature of these networks allowed us a complete knowledge of the actual target thus making these
 313 calculations possible.

314 2.5 Network functionality testing

315 Function testing is commonly achieved, by defining a set of metabolites that are available and can be
 316 excreted and requiring other metabolites to be produced/consumed or a reaction to be able to carry flux.
 317 The input and output can either be cast into a linear problem by adding importers and exporters or by
 318 relaxing the steady state requirement for the imported and exported metabolites. Gille et al. (2010) used
 319 the latter definition and we adapted this approach using the following modification of the standard FBA
 320 approach:

$$\begin{aligned}
 \min \quad & \sum v_i^+ + v_i^- \\
 \text{s.t.} \quad & b_l \leq S' * v' \leq b_u \\
 & 0 \leq v_i^+ \leq ub_i \quad \forall i \in \text{internal reactions} \\
 & 0 \leq v_i^- \leq -lb_i \quad \forall i \in \text{internal reactions} \\
 & v_i^+ - v_i^- = 0 \quad \forall i \in \text{exchange reactions}
 \end{aligned}$$

$$\text{with } S' = [S, -S] \text{ and } v' = \begin{bmatrix} v^+ \\ v^- \end{bmatrix}$$

$$b_{l,i} = \begin{cases} -10000 & \forall i \in \text{imported metabolites}(-/ =) \\ -1 & \forall i \in \text{produced objectives}(+) \\ 1 & \forall i \in \text{consumed objectives}(-) \\ 0 & \text{else} \end{cases}$$

$$\text{and } b_{u,i} = \begin{cases} 10000 & \forall i \in \text{exported metabolites}(+/ =) \\ -1 & \forall i \in \text{produced objectives}(+) \\ 1 & \forall i \in \text{consumed objectives}(-) \\ 0 & \text{else} \end{cases}$$

321

322 The test is considered to be successful if there is a non zero value for all evaluators when calculating
 323 $S' \cdot v'$.

324 2.6 Computational resources

325 Except for RegrEx, all runs using the liver data were performed on two cores of a 2.26Ghz Xeon L5640
 326 processor on the HPC system of the University of Luxembourg (Varrette et al., 2014) to achieve comparable
 327 running times. Tissue comparison runs and artificial simulation runs were performed on the same cluster
 328 but not limited to specific node types.

3 RESULTS

3.1 Characterization of the algorithms

3.1.1 Similarity of the context-specific models and algorithm-related bias

The aim of this characterization step is to categorize the algorithms based on the similarity of their output models in order to gain insight into algorithm-related bias, requirements of the algorithms i.e. thresholds and more importantly when to use which algorithms. In an ideal case, one would expect that when fed with the same input data, the different algorithms would produce similar networks. But when comparing the context-specific liver models generated with the different algorithms and HepatoNet, only 530 reactions were found in all networks and 77 reactions of our version of Recon2 were inactive in all context-specific models and HepatoNet. The 530 reactions were found among 54 different subsystems, including reactions belonging to pathways expected in all tissues like i.e. the Krebs cycle, glycolysis/gluconeogenesis, but also pathways that were described to take place mainly in the liver, like i.e. bile acid synthesis (Wang et al. (2012); Rosenthal and Glew (2009)) or some reactions of the vitamin B6 pathway (pyridoxamine kinase, pyridoxamine 5'-phosphate oxidase and pyridoxamine 5'-phosphate oxidase) (Merrill Jr et al. (1984)). This huge variability is due to workflow-related bias and to different strategies and aims of the algorithms. FASTCORE (Vlassis et al., 2014), expects as input a set of reactions with a high confidence level which are assumed to be active in the context of interest and therefore all core reactions are included in the output model (Table 3). In contrast, FASTCORMICS (Pacheco et al., 2015) only includes a core reaction if it does not require the activation of reactions with low z-scores. The main objective of GIMME (Becker and Palsson, 2008) is to build a model by maximizing a biological function. The input expression data is used to identify, which reactions are not required for the objective and can function therefore be removed from the model due to low expression values (Table 3). iMAT (Zur et al., 2010), Lee et al. (2012) and RegrEx (Robaina Estévez and Nikoloski, 2015) maximize the consistency between the flux and the expression discarding reactions that have high expression values if necessary, which might be problematic if reactions have to be included in the model like i.e. the biomass function. INIT (Agren et al., 2012) uses weighted activity indicators as objective, with those having stronger evidence being weighted higher. Whereas the Akesson's (Åkesson et al., 2004) algorithm aims to eliminate non expressed reactions.

The models, when clustered in function of the Jaccard Similarity Index (Figure 1), form 2 branches and an outlier: HepatoNet. The first cluster is composed of algorithms that take as input continuous data and attempt to maximize the consistency between the data and the Akesson algorithm that eliminates inactive reactions. The second cluster is composed of algorithms that discretize the data in expressed and non-expressed genes. Among this cluster, a second subdivision is observed between the algorithms that used z-score converted data (i.e. FASTCORE z-score and FASTCORMICS) and the ones that use normalized data without further transformation.

Overall the highest similarity level are found between FASTCORE z-score and FASTCORMICS with a score of 85% of similarity followed by iMAT and GIMME with 77% of similarity. The lowest similarity level is found between FASTCORMICS and HepatoNet with only 26% of overlap. The largest overlap between HepatoNet and context-specific reconstructions is found for INIT with 43% of similarity. Note that the INIT model although having as input Barcode discretized data does not cluster with FASTCORE z-score or with the FASTCORMICS models but with RegrEx, suggesting that the choice to consider continuous data rather than defined core set has a larger impact on the output models.

369 As the algorithms were fed with the same input data, reactions that are predicted by one or only few
370 algorithms are more likely to be algorithm-related bias (Figure 2). The Akesson model that contains 98.56%
371 of the input model includes the largest number of reactions (201) that are absent in the others models.

372 The reactions included in the FASTCORE, FASTCORMICS, iMAT and GIMME models are for 97%,
373 98%, 96% respectively 89% supported by at least 3 other algorithms and display a similar profile shifted
374 to the right. HepatoNet, INIT and the Akesson's model share 92%, 83% respectively 91% with 3 other
375 algorithms and have different profiles from the algorithms of the first group composed of algorithm that
376 include a discretization step.

377 In summary, discretization-based algorithms show the highest similarity level and therefore the lowest
378 number of reactions due to potential algorithm-related bias.

379 3.1.2 Sensitivity and Robustness testing using artificial data

380 Since we noticed that there are two sets of algorithms among the discretizing algorithms, we decided to
381 further test their properties with artificial networks by comparing resulting models from multiple runs for
382 different models and levels of completeness of input data.

383 Figure 3 provides the average similarities for all models reconstructed for each target model at different
384 available information percentages. (A full set of mean similarities for each percentage and each artificial
385 model along with the data for the plots is provided in Supplementary File 1). Each square represents the
386 mean Jaccard index of the all combinations of networks generated for different input networks (e.g. (1,2) is
387 the average similarity of all networks generated for models 1 to all networks generated for model 2). The
388 diagonal represents the internal similarity of all networks generated for one model. When 90% of the data
389 is available, all the algorithms are able to distinguish variation between the different models. But with a less
390 complete data set, inclusive algorithms lose in specificity and therefore also progressively lose the capacity
391 to distinguish between different models. Further with 30% and 50% reactions missing, it would be expected
392 that the algorithms get less robust, but Akesson and GIMME only show a modest decrease of robustness
393 (as shown in the diagonal). A similar behaviour for the GIMME algorithm was also described by Machado
394 and Herrgård (2014) in a experiment where noise was progressively added to the input data to finally obtain
395 a random input dataset. GIMME showed the same average error in prediction for the random and original
396 data (Machado and Herrgård, 2014), suggesting that due to the optimization of the biomass function, the
397 expression data has a reduced impact on the model building. Comparing the models resulting from runs
398 with different completeness of input data illustrates that the methods tend to converge on more complete
399 data sets, with the Akesson approach and GIMME being more inclusive and the FASTCORE family being
400 more exclusive (see Figure 4). While initially, with incomplete data, the methods are distinguishable by the
401 networks generated, this difference becomes smaller with additional knowledge.

402 3.1.3 Robustness testing using real data

403 In order to further evaluate the confidence level of the reactions included in the different context-specific
404 models a 5 fold cross-validation was performed. The experiment was repeated 100 times with a different
405 validation set. GIMME, iMAT, and FASTCORMICS show the highest robustness, followed by FASTCORE
406 and FASTCORE z-score (See Table 4). Algorithms that maximize the consistency between the data and the
407 flux, e.g. INIT and RegrEx, are less robust with insignificant p-value. For Akesson no hyper-geometric test
408 was performed as the validation set was too small to obtain a reliable p-value. Note that for context-specific
409 reconstruction algorithms a trade-off has to be found between robustness and the capacity to capture
410 differences between similar contexts. For this reason, a too high robustness might not be desirable as

411 it would imply that the algorithm might lose in resolution power, i.e. the ability to distinguish between
412 different sets of input data. Therefore it is also advisable to not test for robustness without testing the
413 resolution power.

414 **3.2 Benchmarking with real data**

415 3.2.1 Confidence level of the reactions included in the different models

416 As shown by the previous similarity test, there are several alternative approaches to build context-specific
417 models. To assess the confidence level of a reconstruction, one can quantify the confidence level of the
418 reactions included by each algorithm. Context-specific algorithms assume that the higher the reactions
419 associated expression levels, the more likely the reactions to be active. Following this logic, context-specific
420 reconstructions should be enriched for higher expression levels. As the background level is non negligible
421 and highly dependent on the probes, we corrected for probe effect using the Barcode method. The z-scores
422 computed by Barcode translate the number of standard deviations to the intensity distribution of the same
423 genes in an unexpressed state. The z-scores of the genes mapped to the reactions of Recon2 (Thiele
424 et al., 2013), HepatoNet (Gille et al., 2010) and to the context-specific models built by the different
425 algorithms show that the distribution of the z-scores are for most models shifted, as expected, toward
426 higher z-scores values with a significant p-value for all context-specific models except ReGrEX (Robaina
427 Estévez and Nikoloski, 2015). Algorithms that use a discretization method show a larger shift to the
428 right than algorithms that maximize the consistency between the flux and the data. Within this group
429 the FASTCORMICS (Pacheco et al., 2015) shows the most significant shift towards the highest z-score
430 values followed by FASTCORE z-score, GIMME (Becker and Palsson, 2008) and iMAT (Zur et al., 2010).
431 (Figure 5 and Table 5). Surprisingly, the consistent version of HepatoNet (Gille et al., 2010) is associated
432 to slightly higher z-scores than Recon2 (Thiele et al., 2013) but significantly lower than most discretization
433 based automated context-specific reconstructions.

434

435 Further, unlike their competitors, all the discretization-based context-specific reconstructions show an
436 enrichment of genes with a high and medium confidence scores to be expressed at the protein level (Uhlén
437 et al., 2015). A stronger enrichment is observed for FASTCORE z-score and FASTCORMICS with 46%
438 and 50% of the gene associated reactions having a high or medium confidence level Table 6, respectively.
439 GIMME and iMAT include 28% and 30% reaction with high or medium confidence levels, respectively.
440 Again surprisingly, HepatoNet does not show an enrichment for high and medium confidence levels.

441 In summary, discretization-based algorithms include reactions with a higher confidence level at the
442 transcriptomic and proteomic level than their competitors.

443 3.2.2 Comparison between different tissue models

444 The aim of a context-specific algorithm, as indicated by the name, is to build models that capture the
445 metabolism of a cell for a given context and therefore these algorithms have to be able to capture variations
446 in the metabolism of different tissues. To pass the following test, context-specific algorithms not only have
447 to be sensitive (or to have a high resolution power) in order capture metabolic difference between tissues,
448 but the reconstructions for different tissues have to be enriched for high or medium confidence levels
449 based on HPA. The last criteria allows to identify algorithms that build different models based on noise or
450 algorithm-related bias. In order to assess the variation among tissues in HPA, the genes with high, medium
451 and low confidence levels for 48 different tissues were mapped to the input model Recon2, showing that

452 very few reactions have a high or medium confidence level in all tissues. In summary, most reactions with
453 high and medium confidence scores have a more tissue-specific expression (Figure 6).

454 A similar experiment was performed with context-specific reconstructions built by the tested algorithms,
455 in which the number of algorithms that shared a reactions was assessed (see Figure 7). For RegrEX, INIT
456 and Akesson models, the majority of reactions are found in all tissues. For GIMME, most reactions are
457 either tissue-specific or present in all the tissues. In contrast, the models built by the members of the
458 FASTCORE family show a distribution similar to the that obtained in Figure 6 for HPA. For iMAT only 8
459 models could be obtained as the computational demands for the reconstructions of the others tissues surpasses
460 the number of cores available and the maximal running of 5 days. When looking at the confidence levels
461 associated with the 21 different tissue-specific models, FASTCORE z-score and FASTCORMICS show in
462 20 out of 21 the highest percentage of reaction with a high or medium confidence level (see Figure 8). The size
463 of the different tissue metabolic models built by the tested algorithm can be found in the Supplementary
464 File 6).

465 The quality of the tissue-specific models built by the different algorithm were assessed by focusing on
466 selected pathways known to have a more tissue-specific expression, namely bile acid synthesis and heme
467 synthesis. The bile acid synthesis occurs in liver, although one or the other enzyme of the pathways might
468 occasionally be expressed by other tissues (Wang et al. (2012); Rosenthal and Glew (2009)). As expected
469 the FASTCORE family, GIMME and iMAT predicted that the highest fraction of active reactions are found
470 in the liver followed by the foetal liver for the FASTCORE family members and iMAT and by placenta and
471 foetal liver for GIMME. Whereas, the INIT models of skin, bone marrow, corpus, thalamus, pituitary gland
472 and foetal liver had a higher fraction of active reactions than the liver model. 13 out of 36 of the tested
473 Akesson models predicted 90% and more reactions of the bile acid pathway as active. RegrEX predicted a
474 slightly higher fraction in the thalamus than in the liver and a comparable fraction in the ovary, the foetal
475 brain and the corpus (Supplementary File 6, Supplementary File 1).

476 The heme synthesis that occurs mainly in the developing erythrocytes and in the liver (Ajioka et al.
477 (2006)), was given as 100% active by the FASTCORE family and completely inactive by GIMME and
478 iMAT in the liver. But these two algorithms predicted the pathway to be active in other tissues. As a matter
479 fact, all the algorithms predicted the pathway to be active in others tissues than the liver. INIT, RegrEX
480 and Akesson included this pathway in 20, 22 and all tested 36 tissues, respectively. Fewer models of the
481 FASTCORE family contained reactions of this pathway: uterus and thyroid for FASTCORMICS and spleen,
482 placenta, uterus, thyroid, skin, bone marrow, amygdala, lung and foetal liver for FASTCORE.

483 3.3 Benchmarking with artificial data

484 To further evaluate the quality of the algorithms, we also used the artificial data (see Section 3.1.2) to
485 benchmark the algorithms. Comparing the resulting models with the target models, we again see that for
486 more complete input sets, the model quality tends to become more similar (see Figure 9). It is interesting
487 to note that the false discovery rate (FDR) of FASTCORE for higher percentages is similar to those of
488 the inclusive models, while FASTCORMICS achieves a better FDR. This indicates alternative routes
489 to activate reactions. In general, there is again the tradeoff between adding too much or too little. It is
490 however interesting that the exclusive algorithms tend to miss targets and their sensitivity is independent
491 on the size of the target model while this is different on inclusive algorithms. Exclusive algorithms show a
492 better FDR than inclusive algorithms. Further, for smaller target models, the loss in precision of inclusive
493 algorithms (1-FDR) is more pronounced for 50% and 70% of the input data, as the inclusive algorithms
494 tend to overestimate the actual model. Similar to the previous experiment, it would be expected that the

495 sensitivity (robustness) would decrease with an increased percentage of missing data. But the inclusive
496 algorithms show an invariant sensitivity in function of the available data suggesting that the expression data
497 has reduced impact on the model building. The specificity for the exclusive algorithms is independent of
498 the target model size and are less affected by the increased missing data than the inclusive algorithms. The
499 sizes of the different reconstructed models also indicates the trend for convergence, and a figure showing
500 the converging sizes is provided in Supplementary File 1.

501 **3.4 Functionality testing**

502 Functional testing allows us to assess which known functions of a specific tissue are captured by a
503 reconstruction. We used the set of functions defined in HepatoNet and formalized in Section 2.5 for the
504 liver and tested them on all reconstructed networks. We noticed that the success rate of HepatoNet and
505 the generic reconstruction Recon2 are comparable with 244 vs 247 of 310 network tasks and 109 vs 98
506 of 123 physiological tasks for Recon2 and HepatoNet, respectively. The discrepancy with the original
507 publication is likely due to alternative solutions and we noticed that HepatoNet allows free production of
508 NADH and thereby ATP (see Table 2 in Supplementary File 1). The discrepancy between the consistent
509 and inconsistent HepatoNet is due to the formulation of the functionalities, which do not require exchange
510 reactions but modify the b vector, thus generating implicit importers and exporters and allowing inconsistent
511 parts of the network to carry flux. We also noticed an important issue with functional testing: For random
512 models, the larger the models, the higher the functionality score (with $R^2 = 0.869$ and 0.915 for network
513 and physiological functions, respectively). To illustrate this issue, we generated 400 random networks by
514 removing a random number of up to 2000 reactions from the consistent part of Recon2 and subsequently
515 removing all reactions which could no longer carry any flux. We then tested all network and physiological
516 functions on these networks. The results can be seen in Figure 10, for both the network and physiological
517 tests.

518 Blue circles represent the random networks; the consistent HepatoNet and the original HepatoNet are
519 displayed in orange, and show a strong enrichment in functionalities. The higher number of functionalities
520 covered in HepatoNet stems from several reactions which are inconsistent, but can be used in a functional
521 testing as described above. We also marked the models generated using the GEO dataset for liver, which
522 score similar to equally sized random models. One of the main reasons for the strong correlation between
523 model size and successful tests is the amount of “positive” testing. Many tests are concerned with some
524 type of biosynthesis or degradation and a larger model is more likely to be able to fulfil these requirements
525 than a smaller model. But even using e.g. the biomass function (like GIMME) as part of the input, the
526 models do not get significantly better than a random model on expression data for liver. None of the
527 algorithms tested achieves high scores in the functionality test and several algorithms are on the lower end
528 of the random network reference. A plot showing the tests passed by the different algorithms is supplied in
529 Supplementary File 7. tINIT could potentially surpass most other algorithms on this test, as it includes
530 functionality information in its reconstruction routine. However, the formulation of tINIT functions is again
531 slightly different from the formulation in HepatoNet and thus not directly compatible.

4 DISCUSSION

532 The primary aim of this work was to review and discuss the existing validation methods and to propose a
533 unified benchmark for the assessment of context-specific reconstruction algorithms. This benchmark will
534 help to identify potential deficiencies of existing and new algorithms and by such increase the quality of
535 context-specific reconstruction algorithms and the models they generate. Although the tested algorithms

536 were validated by their authors in order to be published, the validation methods applied are often incomplete,
537 e.g. a particular aspect of the output model fitting the context of the paper is tested like the ability to
538 produce lactate from glucose in cancer models, leaving other pathways unconsidered. Further, discretization
539 thresholds and other free parameters of the algorithms are likely to be set to optimally fit a particular
540 dataset. Thus, when used in another context the algorithm might perform worse than expected from the
541 original publication. The need of a unified benchmark is nicely illustrated by Figure 1 which shows that
542 despite being fed with the same inputs, the output models vary considerably from each other e.g. the output
543 models of RegExp and FASTCORE that share only around 30% of the reactions.

544 Part of the variance between the output models is due to different aims and philosophies of the tested
545 algorithms but also due to algorithm-related bias. The second aim of this work was to demonstrate to
546 the users that the context-specific reconstruction algorithms are not equivalent and that the choice of the
547 algorithm and selection of parameter settings for the algorithms have to be performed with care respecting
548 the philosophy of the tested algorithm. For example, GIMME maximizes a chosen biological function
549 and when using GIMME the user assumes that the metabolism of a cell is aimed at the fulfilment of this
550 function. While this biological function can be assumed to be growth for many microorganisms or cancer
551 cells, it is likely to be more complex for multicellular organisms, where multiple “objectives” have to be
552 balanced. In the same way, FASTCORE takes as input core reactions that are always included in the output
553 model and therefore a higher threshold corresponding to a higher confidence level should be set when
554 using FASTCORE.

555 Although the parameters were set according to the original papers, we are aware that some of the tested
556 algorithms might perform better with a different parameter setting. We decided nevertheless when possible
557 not to change the original parameter settings of the algorithm. First, because the main objective of this
558 paper is not to assess existing algorithms but to propose a benchmark to validate context-specific algorithms.
559 Second the finding of the optimal parameter setting is a computational demanding processes that would
560 require i.e. crossvalidations or other criteria that are not always available. Finding the optimal parameter
561 setting is beyond the scope of a benchmark and rises other questions like overfitting to the data. Third,
562 algorithms should be sufficiently robust to be applied to other datasets with the optimal settings as defined
563 by the authors. As a general principle, in order to avoid overfitting, the parameter estimation should not be
564 performed on the same data than the one used for model generation. We therefore encourage the authors
565 and the users of these algorithms to test them with others parameter settings that might be more appropriate.

566 The benchmark that we suggest and for which we provide the scripts (<http://systemsbiology.uni.lu/software>)
567 is based on several criteras:

568 First of all the algorithms have to produce models of high quality that include genes or reactions that
569 are supported by some evidence to be expressed in the context of interest. This aspect was assessed in
570 the workflow by mapping Barcode z-scored gene information and confidence levels established by the
571 Human Protein Atlas to the models. Context-specific reconstruction that extract sub- networks composed
572 only of active reactions in the context of interest from a general reconstruction tend to produce output
573 models that are enriched for genes with high z-scores and a high confidence level to be expressed at the
574 protein level. Indeed although the activity does not correlate perfectly with expression intensities, it was
575 shown that algorithms that exclude reactions with low expression values show a better predictive power
576 than the generic models from which they were extracted. Both tests show that algorithms that perform a
577 discretization of the input data perform better in these tests than algorithms that maximize the consistency
578 between flux values and the data.

579 We noticed that within the discretizing algorithms, there are two conceptually distinct approaches when
580 considering unsupported reactions. An inclusive concept which considers unknown data as present and
581 an exclusive concept that considers unknown data as absent. Inclusive concepts tend to produce larger
582 networks and score lower, when comparing the networks to additional data, while exclusive concepts tend
583 to produce smaller networks and score higher.

584 This can be considered as algorithm related bias and it is likely that when multiple algorithms are supplied
585 with the same inputs, reactions that are found by only one or only few algorithms are more likely to be due
586 to algorithm-related bias. Algorithm related bias is not negligible as shown by the huge variability of liver
587 reconstructions with e.g. up to 30% of the reactions being different between the FASTCORE and ReprExp
588 algorithm (Figure 1).

589 Further, algorithms have to be robust to noise but nevertheless be precise enough to capture the variations
590 in the metabolism of a cell in different contexts i.e. different cell types, different states e.g. healthy versus
591 disease and eventually between different patients. These two criteria were tested using both experimental
592 and artificial data. Algorithms like GIMME are performing extremely well in the cross-validation assay
593 but score low in the tissue comparison test, as GIMME produces quite similar reconstructions for the
594 different tissues tested. The algorithms using an inclusive concept tend to be more robust to noisy data
595 but have a reduced resolution power. In contrast, exclusive algorithm are less robust as they tend to only
596 recover reactions that are supported by the input data or reactions that are needed to obtain a consistent
597 model, which allow a greater resolution power. Therefore among the tested algorithms, the FASTCORE
598 family capture best the variation between the different tissues. Further, the confidence level of the reactions
599 included in the 21 tissue models showed that the variability captured by the FASTCORE family models, was
600 not due to noise or algorithm related bias. In the same aspect, the artificial model test gave some interesting
601 insight into the quality of the reconstruction algorithms. While both groups of algorithms, including and
602 excluding, generated about the same model when perfect information was available, they start to diverge
603 at lower amounts of available data. In particular, with less information available the exclusive algorithms
604 underestimate the target network and the including ones overestimate it. While this is to be expected it
605 indicates that the use of two algorithms can give a good approximation of the quality of the available
606 input data and completeness of the reconstruction. If both types of algorithms (inclusive and exclusive) do
607 diverge substantially, it is likely that a relevant amount of input information is missing and that the “true”
608 model is somewhere in between. Similarly, if the models are almost identical, it is likely that the input
609 information and the reconstruction quality is high. GIMME will always include the objective function
610 and all reactions necessary for this function to carry flux. Therefore, those reactions might influence the
611 network size considerably. One advantage of an exclusive concept in this respect, is that its variability is
612 less target model dependent than an inclusive approach. For smaller models, the FDR for inclusive models
613 tends to rise much more rapidly with a more incomplete input data set than for larger models. As we
614 commonly are unaware of the actual size of the target network, this might cause problems when using
615 inclusive approaches.

616 Another important aspect is the computational demand. To determine the processing time we decided
617 when possible not to change the solver used in the original paper as we noticed that algorithms like e.g.
618 ReprEX are sensitive to the used solver, with gurobi finding an initial solution guess faster than e.g. cplex
619 and thus the result returned by cplex being unusable for the algorithm. The range of computational times
620 is however substantial, with fast algorithms running in seconds to minutes and others taking hours or
621 even days. One of the greatest advantages of faster algorithms, is their capability to be more thoroughly
622 evaluated using cross-validation techniques, which is infeasible for an algorithm running several days. We

623 also observed an issue when running the INIT algorithm. For unknown reasons, the algorithm consistently
624 stopped after 10 hours of computation. In particular, the resulting models were odd at best, as they should
625 be close to the models generated by FASTCORE, and in the artificial test, should be optimal on optimal
626 inputs. However, the artificial test was far from optimal, and we assume that the solver does terminate
627 computation at some point.

628 Finally, we also assessed the capacity of the context-specific reconstruction to pass the functional test as
629 established in (Gille et al., 2010). We found that no algorithm outperforms random models, but that a fitted
630 model can indeed show higher scores without adding more reactions, as seen in Figure 10. Unfortunately,
631 obtaining functional data is a very time consuming process and necessitates intensive literature research
632 every time a new tissue model is created. The failure of the tested algorithms in the functional test is mainly
633 due to the high number of non-gene associated reactions in the generic input model (one third of Recon2)
634 and due to the reactions associated to genes with low expression levels. The tested algorithms extract a
635 sub-network from the input model that includes all or most reactions associated with high expressions
636 levels (core) and few reactions with low expression levels (non-core) in order to obtain a consistent model.
637 A slightly different core reactions set, can cause the core reactions to be connected in a different way
638 and as a result the model displays different functionalities. As the choice of the non-core reactions is to a
639 large extent not guided by the data, the obtained functions are random as shown by the functionality test.
640 Interestingly, the reactions found in HepatoNet do have weak evidence when compared to HPA or z-scores,
641 which partially provides another explanation for the inability of the tested algorithms to recover these
642 activities. This however indicates that the general reconstruction currently used lacks either the correct
643 gene-protein-reaction associations for several reactions necessary for the functionalities in liver, that there
644 are alternative pathways missing in the reconstruction and the reactions used in HepatoNet are not the
645 “true” reactions, that the functions are incorrectly assumed to be available in liver or that the functionality
646 lacks information about the consumed cofactors. Indeed, as all the exchange reactions are closed, some
647 reactions might not carry a flux as the associated cofactor cannot be regenerated. This would also explain
648 why bigger models accumulate more functions. The larger the models, the higher the likelihood of internal
649 loops that could allow a regeneration of cofactors. Further it might also indicate that transcriptomics
650 alone might not be sufficient to build functionally correct models. Information on the uptake and excreted
651 metabolite added to the input reactions set would probably increase the score of most algorithms. We did
652 nevertheless not include this type of information in the input data as the latter is not available for *in vivo*
653 tissues. While presence of importers and exporters does not influence the functional tests, they are however
654 highly influenced by the availability of internal transporters.

655 Assuming that the defined functions are indeed present in liver, this would indicate the importance of
656 algorithms like tINIT which do take these functionalities into account and which could, given the right
657 reference network, indicate potential missing links in the current reconstructions. tINIT is nevertheless
658 not able to capture metabolic differences between different tissue as shown in Uhlén et al. (2015), calling
659 for a new generation of algorithms that capture metabolic variation and that are able to take as input
660 functionalities. Note here that algorithms like PRIME that do not extract a subnetwork to obtain a context-
661 specific model, but modifies the bounds of the reactions of the input model, will have regardless of
662 the modelled cell-type or context the same functionalities as the input model. Therefore PRIME would
663 score as high as the generic Recon2 in a qualitative test. Nevertheless, the approach used by PRIME is
664 extremely dependant on the accuracy of the growth measurement and biomass formulation, leading to a
665 very variable quality of the flux prediction (Yikzah et al, 2014). In a quantitative test aiming to predict the
666 production rate of lactate by cancer cells, PRIME showed a lower correlation to the experimental data than
667 FASTCORMICS (Pacheco et al., 2015). This suggests that building context-specific algorithms with the

668 discretization-based algorithms and then constraining the uptakes rates of several key amino-acids and
669 glucose as performed in (Pacheco et al., 2015) seems to be favourable. Further, as discussed in the main
670 text, there is no unique function to which the metabolism of a non-cancerous pluricellular cell could be
671 reduced and so far is limited to handle one metabolic function.

672 In general, we would recommend to assess the quality of an algorithm based on a combination of
673 functional tests for a reconstructed tissue always in comparison to random networks, confirmation using
674 an independent source of information (e.g. proteomics data, when only using expression data for the
675 reconstruction), and an assessment of algorithmic properties, like dependence on target or input model size
676 and dependence on input data quality. For the latter we would suggest using artificial networks to provide a
677 complete knowledge on the expected outcome.

DISCLOSURE/CONFLICT-OF-INTEREST STATEMENT

678 The authors declare that the research was conducted in the absence of any commercial or financial
679 relationships that could be construed as a potential conflict of interest.

AUTHOR CONTRIBUTIONS

680 MP, TP and TS designed the study. MP and TP implemented the validation methods and performed the
681 calculations. MP, TP and TS wrote the manuscript.

ACKNOWLEDGMENTS

682 *Funding:* TS and TP are funded by the Life Science Research Unit, University of Luxembourg. MPP was
683 supported by a fellowship from the Fond National de la Recherche Luxembourg (AFR 6041230). We
684 would like to thank the HPC team of the University of Luxembourg for their support.

SUPPLEMENTAL DATA

685 Supplementary File 1 - Additional Plots
686 Supplementary File 2 - List of liver arrays
687 Supplementary File 3 - Data underlying the similarity plots of Figure 3
688 Supplementary File 4 - Data underlying the similarity plots of Figure 4
689 Supplementary File 5 - Artificial Models and the Recon and HepatoNet Used in SBML format
690 Supplementary File 6 - The sizes of the models of the different tissues built by the tested algorithms and
691 the fraction of active reactions in each pathway for the different tissues
692 Supplementary File 7 - Successes of the models in the functional tests based on the tests from HepatoNet
693

REFERENCES

694 Agren, R., Bordel, S., Mardinoglu, A., Pornputtpong, N., Nookaew, I., and Nielsen, J. (2012).
695 Reconstruction of genome-scale active metabolic networks for 69 human cell types and 16 cancer
696 types using init. *PLoS Comput Biol* 8, e1002518. doi:10.1371/journal.pcbi.1002518

- 697 Agren, R., Mardinoglu, A., Asplund, A., Kampf, C., Uhlen, M., and Nielsen, J. (2014). Identification of
698 anticancer drugs for hepatocellular carcinoma through personalized genome-scale metabolic modeling.
699 *Mol Syst Biol* 10, 721
- 700 Ajioka, R. S., Phillips, J. D., and Kushner, J. P. (2006). Biosynthesis of heme in mammals. *Biochimica et*
701 *Biophysica Acta (BBA)-Molecular Cell Research* 1763, 723–736
- 702 Åkesson, M., Förster, J., and Nielsen, J. (2004). Integration of gene expression data into genome-scale
703 metabolic models. *Metabolic engineering* 6, 285–293
- 704 Barrett, T., Wilhite, S. E., Ledoux, P., Evangelista, C., Kim, I. F., Tomashevsky, M., et al. (2013).
705 Ncbi geo: archive for functional genomics data sets–update. *Nucleic Acids Res* 41, D991–D995.
706 doi:10.1093/nar/gks1193
- 707 Becker, S. A. and Palsson, B. Ø. (2008). Context-specific metabolic networks are consistent with
708 experiments. *PLoS computational biology* 4, e1000082
- 709 Colijn, C., Brandes, A., Zucker, J., Lun, D. S., Weiner, B., Farhat, M. R., et al. (2009). Interpreting
710 expression data with metabolic flux models: Predicting *Mycobacterium tuberculosis*
711 mycolic acid production. *PLoS Comput Biol* 5, e1000489. doi:10.1371/journal.pcbi.1000489
- 712 Duarte, N. C., Becker, S. A., Jamshidi, N., Thiele, I., Mo, M. L., Vo, T. D., et al. (2007). Global
713 reconstruction of the human metabolic network based on genomic and bibliomic data. *Proceedings of*
714 *the National Academy of Sciences of the United States of America* 104, 1777–1782. doi:10.1073/pnas.
715 0610772104
- 716 Edgar, R., Domrachev, M., and Lash, A. E. (2002). Gene expression omnibus: Ncbi gene expression and
717 hybridization array data repository. *Nucleic Acids Research* 30, 207–210. doi:10.1093/nar/30.1.207
- 718 Folger, O., Jerby, L., Frezza, C., Gottlieb, E., Ruppin, E., and Shlomi, T. (2011). Predicting selective drug
719 targets in cancer through metabolic networks. *Mol Syst Biol* 7, 501. doi:10.1038/msb.2011.35
- 720 Ge, X., Yamamoto, S., Tsutsumi, S., Midorikawa, Y., Ihara, S., Wang, S. M., et al. (2005). Interpreting
721 expression profiles of cancers by genome-wide survey of breadth of expression in normal tissues.
722 *Genomics* 86, 127–141
- 723 Gille, C., Bölling, C., Hoppe, A., Bulik, S., Hoffmann, S., Hübner, K., et al. (2010). Hepatonet1: a
724 comprehensive metabolic reconstruction of the human hepatocyte for the analysis of liver physiology.
725 *Molecular Systems Biology* 6, 411. doi:10.1038/msb.2010.62
- 726 Jerby, L., Shlomi, T., and Ruppin, E. (2010). Computational reconstruction of tissue-specific metabolic
727 models: application to human liver metabolism. *Molecular Systems Biology* 6
- 728 Lee, D., Smallbone, K., Dunn, W. B., Murabito, E., Winder, C. L., Kell, D. B., et al. (2012). Improving
729 metabolic flux predictions using absolute gene expression data. *BMC systems biology* 6, 73
- 730 Machado, D. and Herrgård, M. (2014). Systematic evaluation of methods for integration of transcriptomic
731 data into constraint-based models of metabolism. *PLoS Comput Biol* 10, e1003580. doi:10.1371/journal.
732 pcbi.1003580
- 733 Mardinoglu, A., Agren, R., Kampf, C., Asplund, A., Nookaew, I., Jacobson, P., et al. (2013). Integration
734 of clinical data with a genome-scale metabolic model of the human adipocyte. *Mol Syst Biol* 9, 649.
735 doi:10.1038/msb.2013.5
- 736 Mardinoglu, A., Agren, R., Kampf, C., Asplund, A., Uhlen, M., and Nielsen, J. (2014). Genome-scale
737 metabolic modelling of hepatocytes reveals serine deficiency in patients with non-alcoholic fatty liver
738 disease. *Nat Commun* 5, 3083. doi:10.1038/ncomms4083
- 739 McCall, M. N., Uppal, K., Jaffee, H. A., Zilliox, M. J., and Irizarry, R. A. (2011). The gene expression
740 barcode: leveraging public data repositories to begin cataloging the human and murine transcriptomes.
741 *Nucleic acids research* 39, D1011–D1015

- 742 Merrill Jr, A. H., Henderson, J. M., Wang, E., McDonald, B. W., and Millikan, W. J. (1984). Metabolism
743 of vitamin b-6 by human liver. *The Journal of nutrition* 114, 1664–1674
- 744 Pacheco, M. P., John, E., Kaoma, T., Heinäniemi, M., Nicot, N., Vallar, L., et al. (2015). Integrated
745 metabolic modelling reveals cell-type specific epigenetic control points of the macrophage metabolic
746 network. *BMC Genomics* 16, 809. doi:10.1186/s12864-015-1984-4
- 747 Quek, L.-E., Dietmair, S., Hanscho, M., Martínez, V. S., Borth, N., and Nielsen, L. K. (2014). Reducing
748 recon 2 for steady-state flux analysis of hek cell culture. *J Biotechnol* 184, 172–178. doi:10.1016/j.
749 jbiotec.2014.05.021
- 750 Robaina Estévez, S. and Nikoloski, Z. (2014). Generalized framework for context-specific metabolic
751 model extraction methods. *Front Plant Sci* 5, 491. doi:10.3389/fpls.2014.00491
- 752 Robaina Estévez, S. and Nikoloski, Z. (2015). Context-specific metabolic model extraction based on
753 regularized least squares optimization. *PLoS One* 10, e0131875. doi:10.1371/journal.pone.0131875
- 754 Rosenthal, M. and Glew, R. (2009). *Medical biochemistry: human metabolism in health and disease*
- 755 Ryu, J. Y., Kim, H. U., and Lee, S. Y. (2015). Reconstruction of genome-scale human metabolic models
756 using omics data. *Integr. Biol.* doi:10.1039/c5ib00002e
- 757 Schellenberger, J., Que, R., Fleming, R. M. T., Thiele, I., Orth, J. D., Feist, A. M., et al. (2011). Quantitative
758 prediction of cellular metabolism with constraint-based models: the COBRA Toolbox v2.0. *Nat Protoc*
759 6, 1290–1307
- 760 Schomburg, I., Chang, A., Placzek, S., Shngen, C., Rother, M., Lang, M., et al. (2013). Brenda in 2013:
761 integrated reactions, kinetic data, enzyme function data, improved disease classification: new options
762 and contents in brenda. *Nucleic Acids Res* 41, D764–D772. doi:10.1093/nar/gks1049
- 763 Shlomi, T., Cabili, M. N., Herrgård, M. J., Palsson, B. Ø., and Ruppín, E. (2008). Network-based prediction
764 of human tissue-specific metabolism. *Nat Biotechnol* 26, 1003–1010. doi:10.1038/nbt.1487
- 765 Shlomi, T., Cabili, M. N., and Ruppín, E. (2009). Predicting metabolic biomarkers of human inborn errors
766 of metabolism. *Mol Syst Biol* 5, 263. doi:10.1038/msb.2009.22
- 767 Thiele, I., Swainston, N., Fleming, R. M. T., Hoppe, A., Sahoo, S., Aurich, M. K., et al. (2013). A
768 community-driven global reconstruction of human metabolism. *Nature Biotechnology* 31, 419–425.
769 doi:10.1038/nbt.2488
- 770 Uhlén, M., Fagerberg, L., Hallström, B. M., Lindskog, C., Oksvold, P., Mardinoglu, A., et al. (2015).
771 Proteomics. tissue-based map of the human proteome. *Science* 347, 1260419. doi:10.1126/science.
772 1260419
- 773 Varrette, S., Bouvry, P., Cartiaux, H., and Georgatos, F. (2014). Management of an academic hpc cluster:
774 The ul experience. In *Proc. of the 2014 Intl. Conf. on High Performance Computing & Simulation*
775 (*HPCS 2014*) (Bologna, Italy: IEEE)
- 776 Vlassis, N., Pires Pacheco, M., and Sauter, T. (2014). Fast reconstruction of compact context-specific
777 metabolic network models. *PLoS Computational Biology* 10, e1003424. doi:10.1371/journal.pcbi.
778 1003424
- 779 Wang, Y., Eddy, J. A., and Price, N. D. (2012). Reconstruction of genome-scale metabolic models for 126
780 human tissues using mcadre. *BMC Systems Biology* 6, 153. doi:10.1186/1752-0509-6-153
- 781 Yizhak, K., Gaude, E., Le Dévédec, S., Waldman, Y. Y., Stein, G. Y., van de Water, B., et al. (2014).
782 Phenotype-based cell-specific metabolic modeling reveals metabolic liabilities of cancer. *Elife* 3.
783 doi:10.7554/eLife.03641
- 784 Zilliox, M. J. and Irizarry, R. A. (2007). A gene expression bar code for microarray data. *Nature methods*
785 4, 911–913

786 Zur, H., Ruppin, E., and Shlomi, T. (2010). imat: an integrative metabolic analysis tool. *Bioinformatics* 26,
787 3140–3142

FIGURES

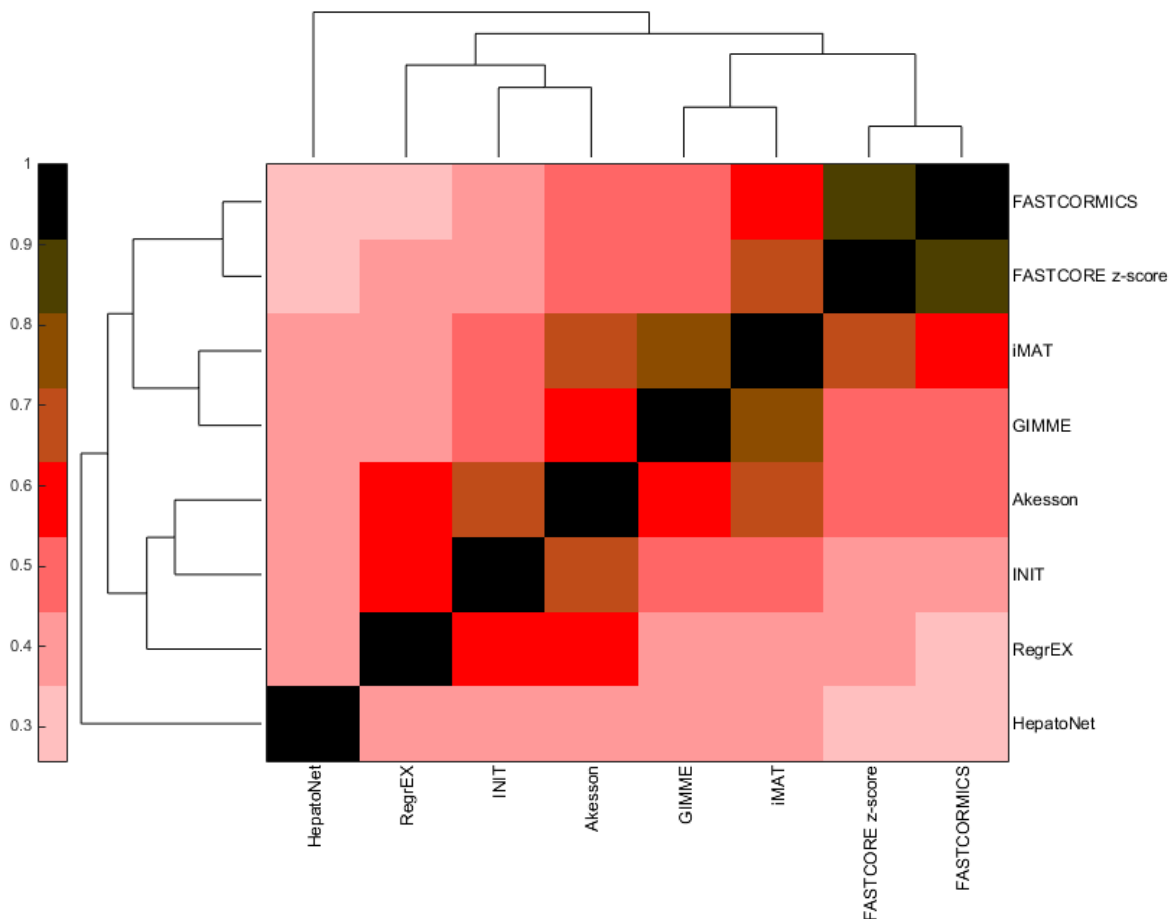


Figure 1. Similarity index of the models built by the different algorithms. The Jaccard index was computed for each pair of models, the rows and column were then clustered in function of the euclidean distance. Contrary to what was expected, the output models of the tested algorithms, despite having been fed with the same input show a huge variability. The descrition-based algorithms (GIMME, iMAT, Akesson, FASTCORE and FASTCORMICS) show the highest similarity levels.

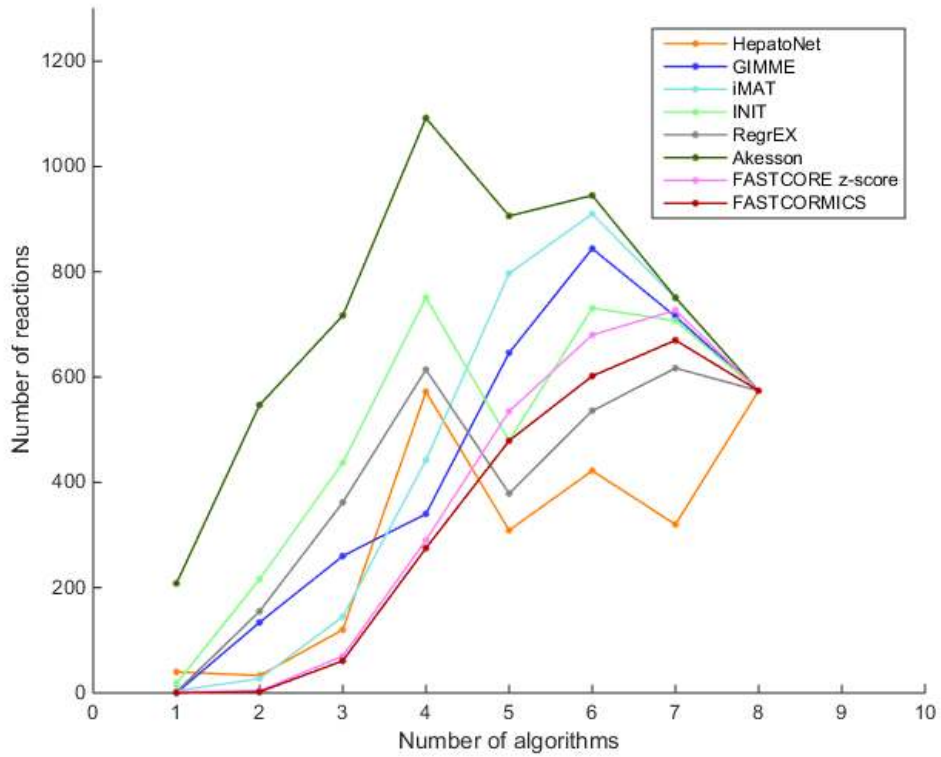


Figure 2. Reactions overlap: The number of reactions that are shared by the models built by the tested algorithms. Each line represents HepatoNet or a model built by one of the tested algorithm. The plot illustrates the number of reactions that are common to 1, 2, 3 up to all of the models.

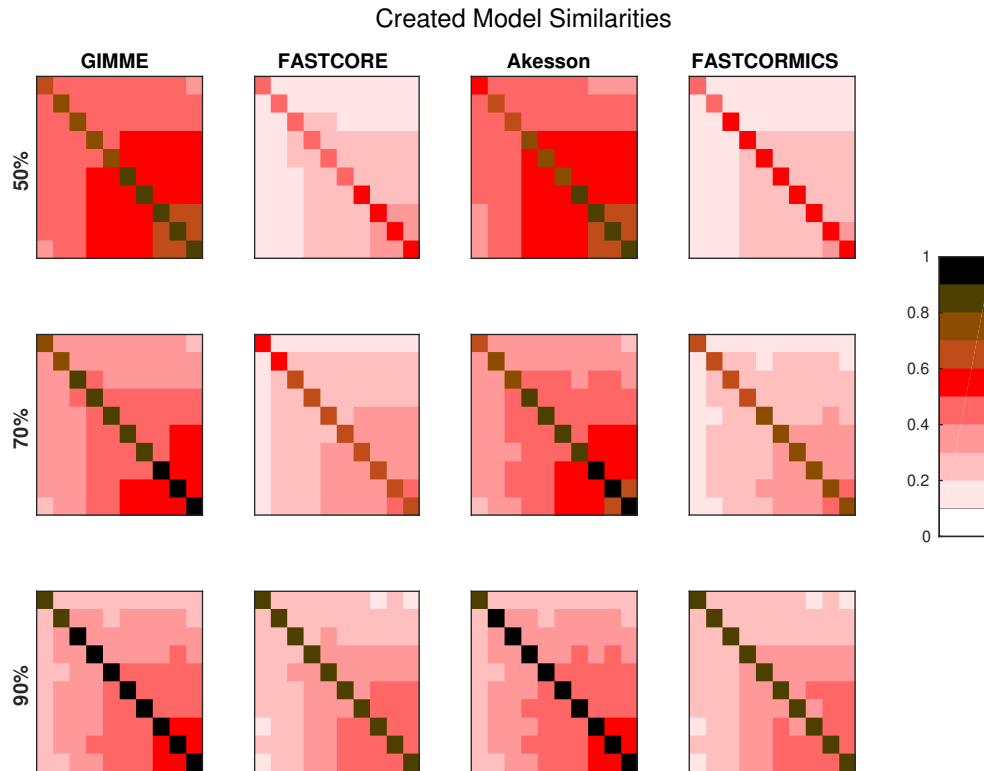


Figure 3. Resolution power: The plot shows Jaccard distances for the networks generated by the algorithms, when trying to create the artificial networks. For each of the ten artificial models 100 runs were performed and each square represents the mean Jaccard distance between these networks. E.g. For each percentage and algorithm, the tenth square in the first row is the mean of all pairwise Jaccard distances between the 100 models generated for artificial model 1 (the smallest) and the 100 models generated for artificial model 10 (the largest) generated for the respective algorithm and percentage. The diagonal is the mean of the pairwise Jaccard distances between 100 runs performed. The diagonal can therefore be an indicator for robustness (the brighter, the more similar the models) while the off diagonal indicates similarities between the generated models and is therefore an indicator for specificity to the input (the darker, the more distinct the generated models). When 90% of the data is available, all the algorithms are able to distinguish variations between the different models. But with a less complete data set, inclusive algorithms (here GIMME and Akesson) lose in specificity. It would also be expected that when only 50% of the data is available, the robustness decreases.

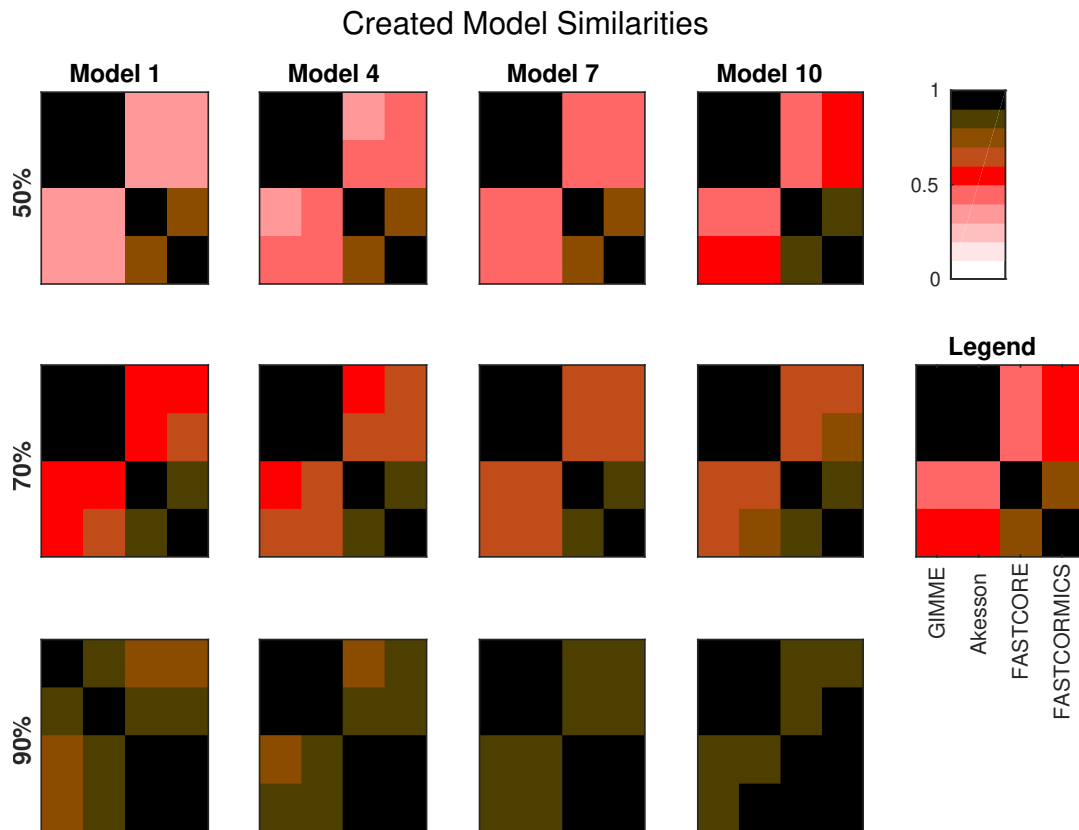


Figure 4. The plots show the mean Jaccard distance between the networks generated by the different algorithms for several artificial models and input percentages. For each algorithm, the corresponding networks (using the same input data) are compared. The models are provided in Supplementary File 5. Sizes are: Model 1: 961; Model 4: 1876; Model 7: 2629; Model 10: 3455. Smaller models (e.g. Model 1) tend to yield more distinguishable results, while larger models (due to a larger fraction of common reactions), tend to yield more similar networks. Overall, the difference between inclusive (GIMME/Akesson) and exclusive (Fastcore/FASTCORMICS) algorithms is clearly visible.

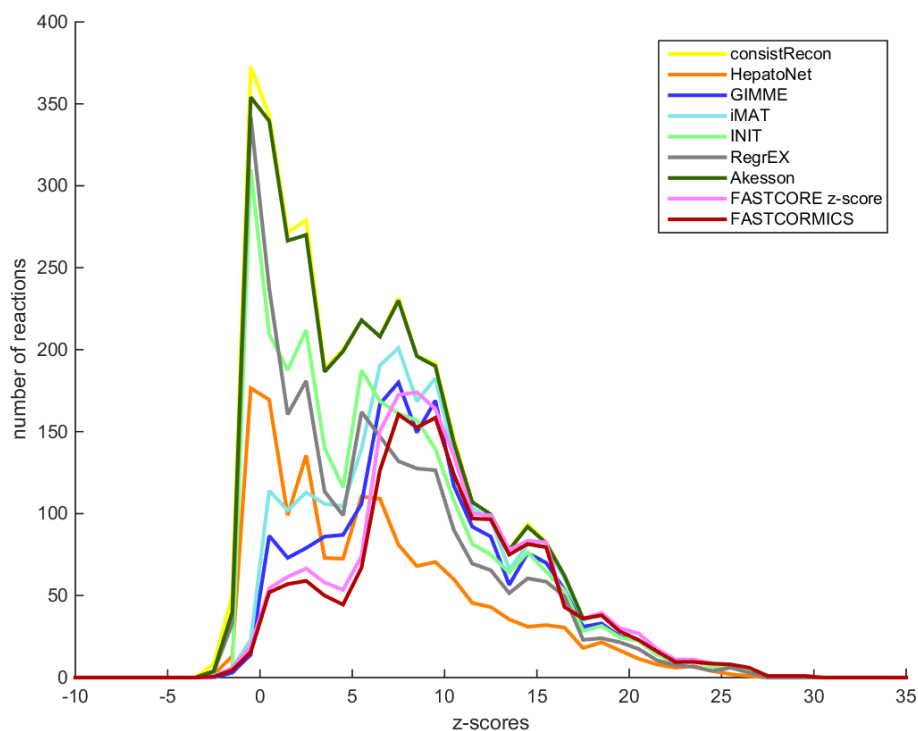


Figure 5. Confidence score at the transcriptomic level: Median z-score of the intensity measured in the liver samples to the median intensity distribution for the genes in an unexpressed context mapped the genes-associated reactions of Recon2 (yellow), HepatoNet (orange) the GIMME (dark blue), iMAT (light blue), INIT (green), RegrEX (gray), Akesson (dark green), FASTCORE z-score (pink) and FASTCORMICS (brown) Discretization-based algorithms (GIMME, iMAT, FASTCORE and FASTCORMICS) are enriched for higher z-score values.

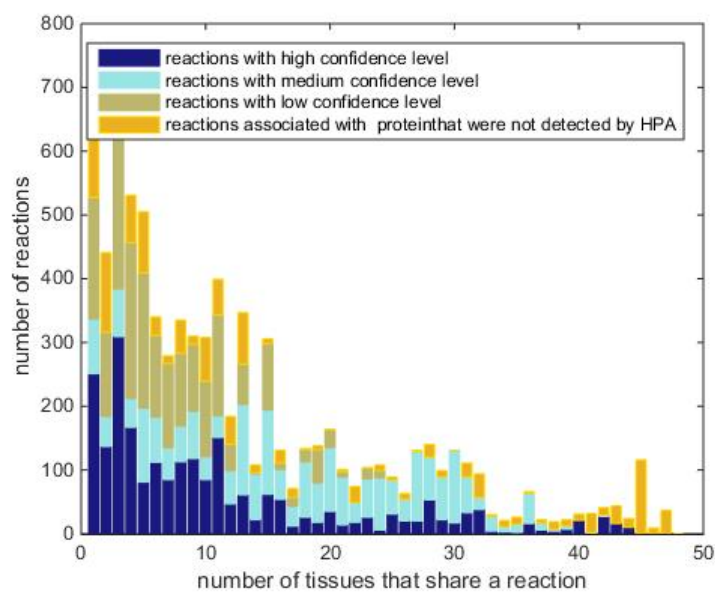


Figure 6. Ubiquity of expression: Number of reactions of Recon2 with a high or medium confidence level that are shared between 1, 2, 3 up to 48 tissues of the Human Protein Atlas. Reactions with a high confidence level tend to have a tissue-specific expression.

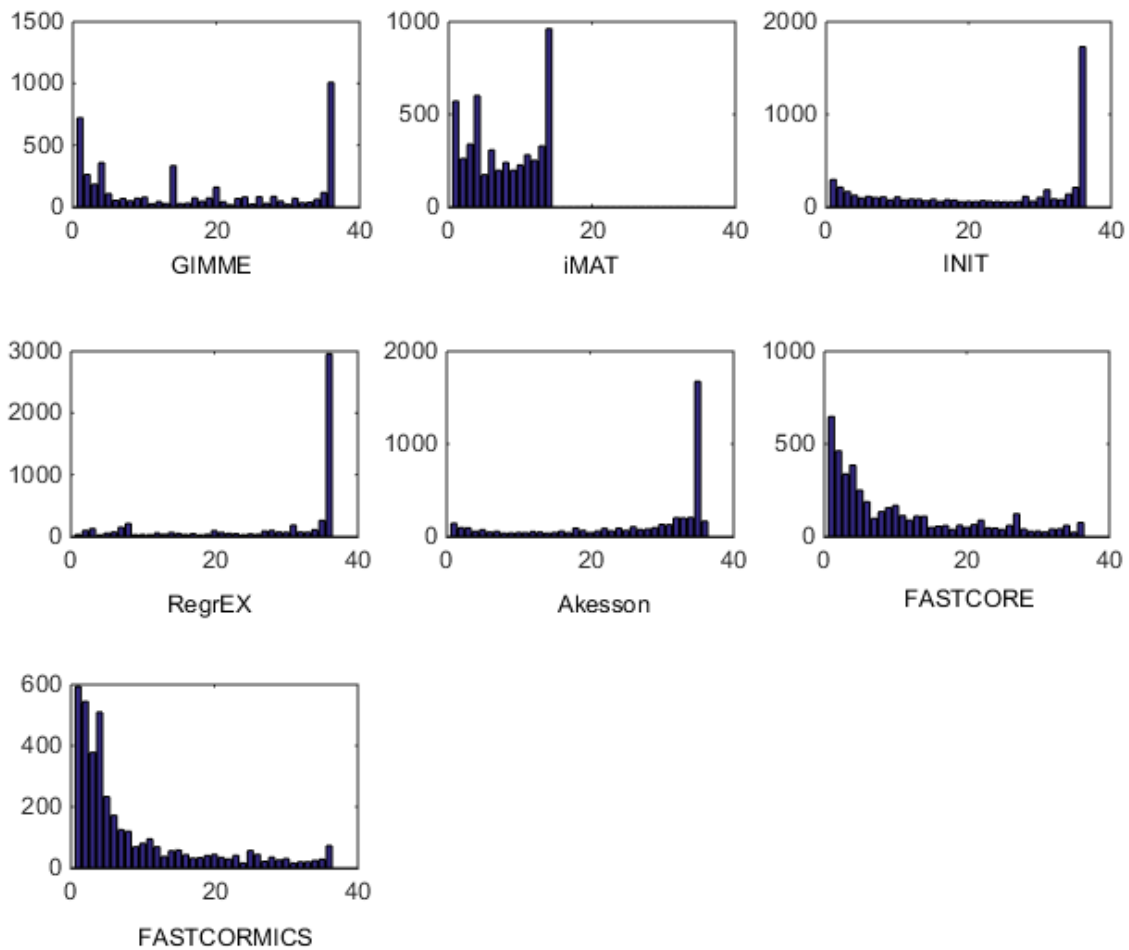


Figure 7. Tissue specificity of reconstructed models. Number of reactions that are present in 1, 2, 3 up to 36 tissues models. For INIT and RegrEX, more than 1500 and 3000 reactions are present in all tissues models, while a similar number is present in all but one model created by the Akesson method. Due to computational complexity of iMAT it was only possible to generate 14 out of 36 tissue models.

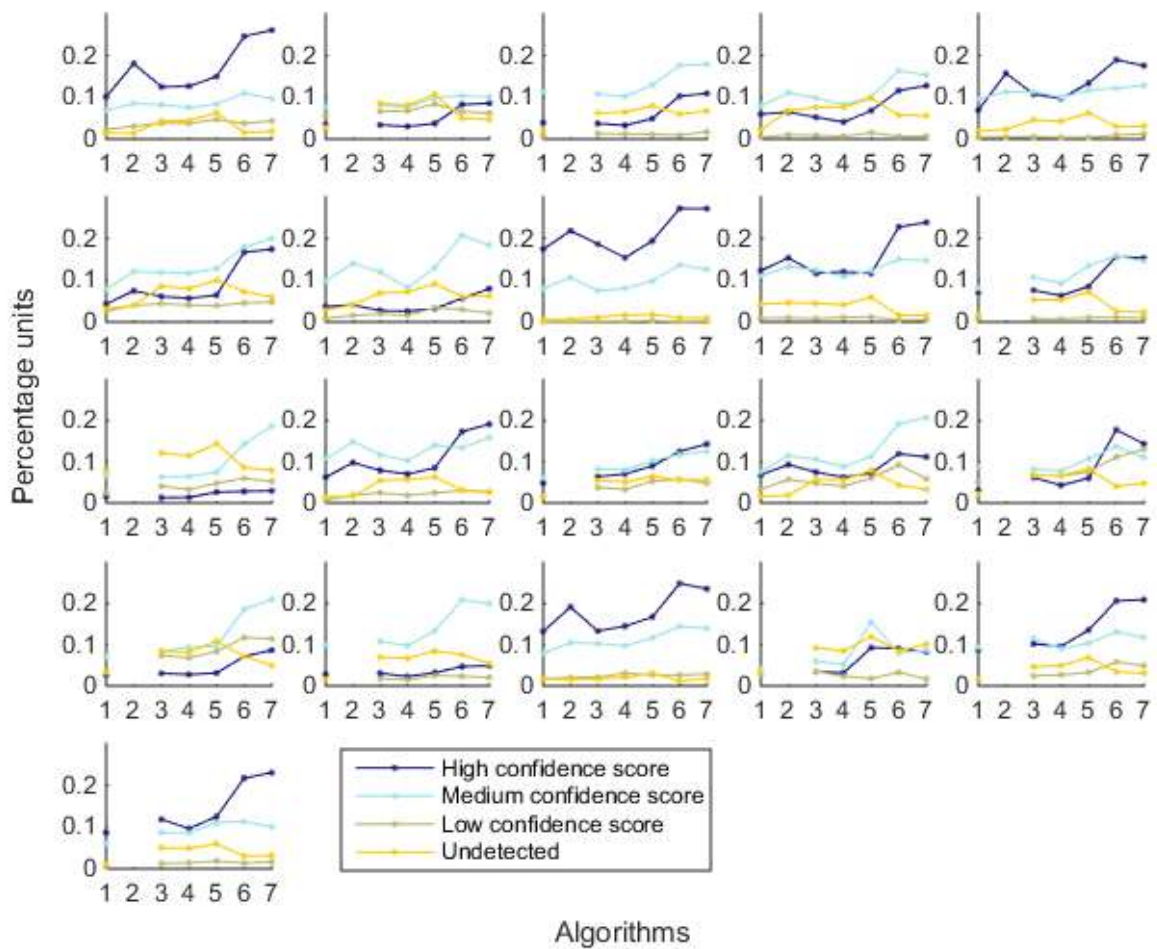


Figure 8. Percentage of reactions that are associated with high confidence (dark blue), medium confidence level (light blue), low confidence level (khaki) and not detected (yellow). Each subplot represent a different tissue. The x-axis represent the different algorithms: 1-GIMME, 2-iMAT, 3-INIT, 4-RegrEX, 5-Akesson, 6-FASTCORE z-score and 7-FASTCORMICS and the y-axis the percentage of reactions.

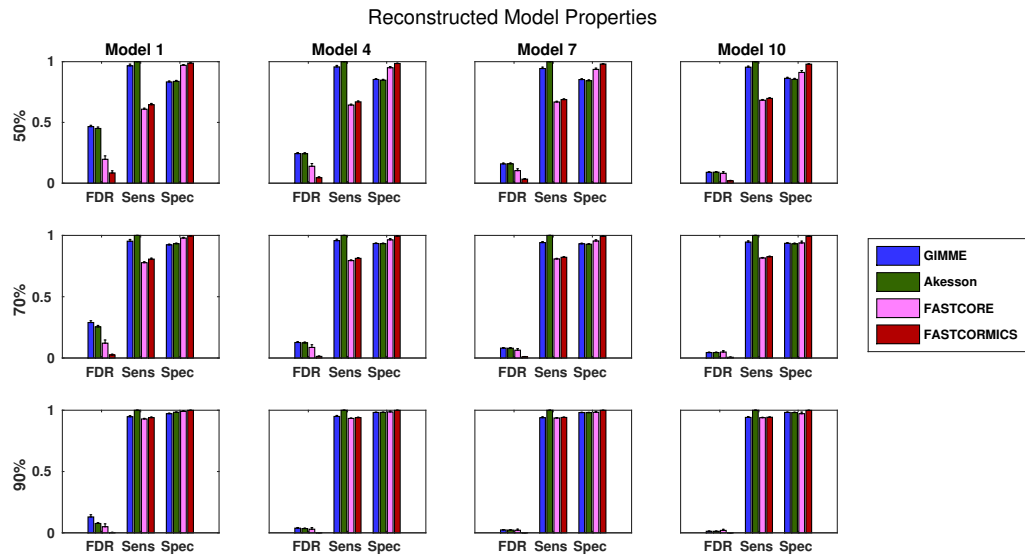


Figure 9. Quality measurements of the algorithms. FDR - False discovery rate, Spec - Specificity, Sens - Sensitivity. Data shown is a the mean of 100 runs for each model/input data. The model sizes are: Model 1: 961, Model 4: 1876, Model 7:2629, Model 10: 3455

While the quality of the FASTCORE models is independent of the target model size, the inclusive approaches tend to largely overestimate smaller models, when insufficient data is available. A plot with all Models can be found in Supplementary File 1.

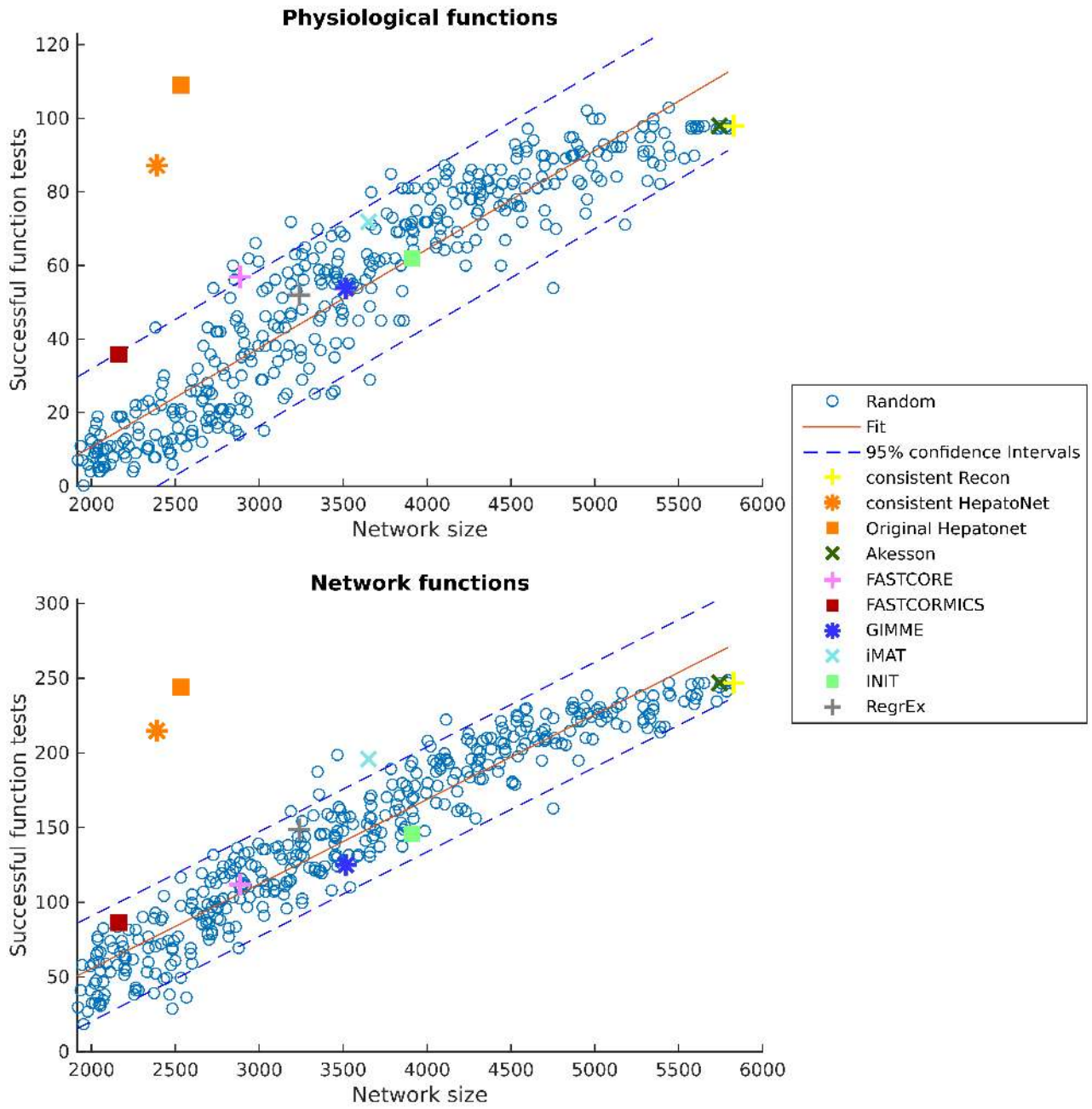


Figure 10. Scores in the physiological tests correlate with the size of the network. 260 Random Networks are shown with blue circles.

Method	Used by
Consistency testing	
Cross validation Diversity of generated models	PRIME, FASTCORE, MBA, FASTCORMICS, iMAT GIMME, mCADRE, tINIT, FASTCORMICS
Comparison based testing	
Comparison with manually curated network Comparison with additional databases Comparison with shRNA knockdown screens Comparison with literature mining Comparison with metabolic exchange rates Comparison with known metabolic functions	INIT, MBA mCADRE, RegrEx, iMAT MBA, FASTCORMICS iMAT PRIME MBA, mCADRE, FASTCORE

Table 1. Overview of methods used for validation of automated tissue specific reconstruction algorithms.

Algorithm	Input	Publication
Akesson04	Set of inactive genes	Åkesson et al. (2004)
FASTCORE	Set of active reactions	Vlassis et al. (2014)
FASTCORMICS	Gene expression data	Pacheco et al. (2015)
GIMME	Gene expression data, objective function	Becker and Palsson (2008)
GIM ³ E	Gene expression data, metabolomics data, objective function	Becker and Palsson (2008)
iMAT	Gene expression data	Zur et al. (2010)
INIT	Gene expression data and metabolite presence data	Agren et al. (2012)
MBA	High, medium and low reaction sets	Jerby et al. (2010)
mCADRE	Gene expression data	Wang et al. (2012)
PRIME	Growth rates, gene expression data	Yizhak et al. (2014)
RegrEx	Gene expression data	Robaina Estévez and Nikoloski (2015)
tINIT	Gene expression data, functions, metabolite presence	Agren et al. (2014)

Table 2. Algorithms available for tissue specific metabolic network reconstruction. Most methods can use expression data as input but there are some that need additional inputs.

Table 3. Models numerics: Size, number of input reactions with high expression respectively z-score levels, fractions of input reactions set included in the output models, number of genes-associated reactions in the model and running time. *Note that RegrEx was run on a different computer with an Intel(R)Xeon(R)CPU E3 1241-v3 @ 3.50 GHz processor

Model	Size	Input reactions	Gene-associated reactions	Time in seconds
GIMME	3513	2441	2087	4458
iMAT	3649	2441	2440	2098
INIT	3913	2020	2787	36002
RegrEx*	3239	1626	2576	64
Akesson	5740	1594	3715	54
FASTCORE z-score	2882	1595	2084	17
FASTCORMICS	2663	1595	1906	112

TABLES

Table 4. Number and percentage of reactions recovered from the validation set, average model size over 100 reconstruction processes

	Validation Set	Recovered reactions	% of Recovered reactions	Sample size	Input	hypergeometric p-value
GIMME	488	408 (6.42)	83.57%	1878 (6.42)	3871	$< 1e - 100$
iMAT	488	335 (10.85)	68.68%	1631 (29.85)	3871	$< 1e - 100$
INIT	345 (7.16)	83.7	24.26%	1931 (113.63)	4469 (7.16)	1
RegrEX	326 (12.79)	160 (19.25)	48.9%	2528 (201)	4524 (12.79)	0.96
Akesson	4	0.98 (1.41)	24.5%	5343 (6.54)	5828 (24.5)	ND
FASTCORE z-score	319	121.6 (8.26)	38.12%	1332 (27.33)	4548	0.0051
FASTORMICS without medium	335(0.4)	192(7.79)	57.14%	1516 (27.13)	4782 (7.57)	1e-18

Table 5. Comparison between the z-score distribution associated to the models build by the different methods. The p-values indicate the likelihood that the z-score associated with the model on the left side is larger than the one on the right side of the table.

Model 1	Model	KS p-value
FASTCORE z-score	FASTCORMICS	1e-10
GIMME	FASTCORE z-score	3e-111
iMAT	GIMME	2e-24
INIT	iMAT	$< 1e - 100$
HepatoNet	INIT	9 e-18
Akesson	Hepatonet	6e-20
consistRecon	Akesson	0.04
RegRexp	consistRecon	3e-14

Table 6. Number, percentage of gene-associated reactions and percentage of reactions of each context-specific reconstruction that have a high, medium and low confidence score to be expressed at the protein level. An enrichment in high and medium confidence level is observed for discretization-based algorithms (GIMME, iMAT, FASTCORE z-score and FASTCORMICS).

algorithms	description	high	medium	low	not detected
Recon	number of reactions	628	641	65	265
	% of the reactions of the model	11 %	11 %	1 %	5 %
	% of the gene-associated reactions	17 %	17 %	2 %	7 %
HepatoNet	number of reactions	213	266	47	108
	% of the reactions of the model	9 %	11 %	2 %	5 %
	% of the gene-associated reactions	12 %	15 %	3 %	6 %
GIMME	number of reactions	518	444	47	126
	% of the reactions of the model	15 %	13 %	1 %	4 %
	% of the gene-associated reactions	25 %	21 %	2 %	6 %
iMAT	number of reactions	574	525	55	153
	% of the reactions of the model	16 %	14 %	2 %	4 %
	% of the gene-associated reactions	24 %	22 %	2 %	6 %
iNIT	number of reactions	453	499	55	155
	% of the reactions of the model	12 %	13 %	1 %	4 %
	% of the gene-associated reactions	16 %	18 %	2 %	6 %
RegrEX	number of reactions	376	418	41	186
	% of the reactions of the model	12 %	13 %	1 %	6 %
	% of the gene-associated reactions	15 %	16 %	2 %	7 %
Akesson08	number of reactions	624	637	64	260
	% of the reactions of the model	11 %	11 %	1 %	5 %
	% of the gene-associated reactions	17 %	17 %	2 %	7 %
FASTCORE z-score	number of reactions	584	413	21	123
	% of the reactions of the model	20 %	14 %	1 %	4 %
	% of the gene-associated reactions	28 %	20 %	1 %	6 %
FASTCORMICS	number of reactions	570	391	15	73
	% of the reactions of the model	21 %	15 %	1 %	3 %
	% of the gene-associated reactions	30 %	21 %	1 %	4 %